

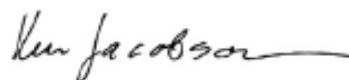
The Role of Non-muscle Myosin II in Detachment-induced Cell Rounding

By
James Zhiren Zhu

Senior Honors Thesis
Department of Biology
University of North Carolina at Chapel Hill

April 21, 2016

Approved:



Prof. Ken Jacobson, Thesis Advisor



Prof. Maryna Kapustina, Thesis Advisor

This thesis has been prepared in conjunction with BIOL692H and in partial satisfaction of the requirements for graduation from UNC-Chapel Hill with research honors.

Abstract

The majority of mammalian cells used by researchers are grown and studied while attached to flat surfaces, resulting in a flat morphology. Although cells grow well and are easy to handle when attached to rigid surfaces, cells *in vivo* live within flexible three-dimensional matrices and often develop different morphologies compared to cells in a petri dish. In particular, stem cells and cells undergoing division are much more round in shape. Although researchers routinely cause cell rounding by detaching cells with trypsin as a part of standard tissue culture protocol, the process of cell rounding has not been extensively studied. Here, we study the roles of non-muscle myosin II heavy chain isoforms A and B (NMIIA/B) in cell rounding using fluorescent labelling in conjunction with traction force microscopy and fixed and live-cell imaging. Results from traction force microscopy show that cells exert an inward pulling force before detaching and rounding. Immunofluorescence results indicate that the degree of colocalization between actin and NMIIA or NMIIIB changes when spread cells are induced to round by detachment. Live imaging of cells rounded with trypsin and also treated with blebbistatin showed that myosin II is required for normal cell rounding. These results indicate that detachment-induced cell rounding is not a purely passive process. Instead, non-muscle myosin II drives detachment-induced rounding, with the isoforms NMIIA and NMIIIB possibly performing different functions. These findings will help further understanding of the regulation of cell shape in response to detachment, helping to describe how cells such as cancer stem cells and leukocytes form their rounded shapes.

Introduction

Laboratories working with mammalian cells grow these cells in petri dishes or flasks. Most cells lines are grown attached to the bottom of containers, making it convenient to treat the cells with different reagents without losing the cells. As a result, researchers tend to make observations on cells attached to glass, which often do not resemble the morphology of cells in vivo. Cells spread and flatten to different degrees when growing on surfaces with different elasticity.¹ Most cells in the human body live within flexible three-dimensional structures that bear little resemblance to flat, inflexible glass. Furthermore, a number of interesting cell types, such as stem cells, lymphocytes, and cells undergoing mitosis are rounded in shape and can exist completely suspended in a fluid.

Cell detachment and rounding via trypsinization is a part of standard tissue culture protocol. However, the complete mechanism of cell rounding by detachment remains unclear. Past research efforts have uncovered various aspects of mitotic cell rounding.^{2,3} It is known that the actomyosin cortex is needed to generate inward forces required for this type of rounding.³ Whereas mitotic rounding leads to partial detachment of the cell from its substrate,² detachment, in the form of trypsin treatment, also causes rounding. I hypothesize that the mechanism of detachment-induced rounding involves the same force-generating proteins as mitotic rounding, namely, the isoforms of non-muscle myosin II.

Non-muscle myosin II (NMII) has three isoforms (NMIIA, NMIIB, and NMIIC) in mammalian cells, with different heavy chains that can polymerize into bipolar filaments which can exert force by binding and pulling polymerized actin.⁴ NMIIA and NMIIB are the most prevalent isoforms in most cells.⁴ The NMIIA and NMIIB isoforms have overlapping yet

different distributions in moving cells, with NMIIA more concentrated on the leading edge of cell movement and NMIIB more concentrated toward the rear of the cell.⁵ I hypothesize that NMII is required for detachment-induced cell rounding, with NMIIA and NMIIB each playing different roles.

To test the hypothesis, the forces cells exerted on their substrates during rounding were visualized using traction force microscopy with elastic substrates containing fluorescent beads. The effects of several drugs on the ability of cells to round after detachment were observed using live cell imaging. The distributions of NMIIA and NMIIB in spread and rounded Chinese hamster ovary (CHO) cells were analyzed by immunofluorescence followed by co-localization analysis. Traction force microscopy results indicate that detaching cells exert inward tractions on its substrate before releasing the substrate, implying that detachment-induced rounding is an active process. Inhibition by blebbistatin resulted in significantly slower rounding events compared to the control, indicating that NMII plays a major part in detachment-induced rounding. Co-localization analysis of immunofluorescence results shows that NMIIA and NMIIB co-localized to a greater degree in rounded versus spread cells; however, at the peripheries of cells, NMIIA and NMIIB became less correlated in rounded cells. Further experiments are needed to uncover the mechanism of detachment-induced rounding and the roles of NMIIA and NMIIB.

Materials and Methods

Immunofluorescence

CHO cells were plated in glass-bottom 35 mm cell culture dishes (MatTek) and incubated at 37 °C for 24 hours to allow the cells to spread. A large number of CHO cells ($\sim 5 \times 10^6$) were detached using trypsin, neutralized and homogenized with growth medium, then added to each dish. The cells were incubated for ~ 15 min to allow some of the added rounded cells to attach to the dish before fixation with 4% paraformaldehyde. The fixed cells were permeabilized with 0.1% saponin (Alfa Aesar J63209), blocked with appropriate serums, and incubated overnight with anti-non-muscle myosin IIA and anti-non-muscle myosin IIB primary antibodies (Abcam ab24762, ab684). Cells were incubated with secondary antibodies (Molecular Probes A11008, A21236) and Alexa568-conjugated phalloidin (Molecular Probes A12380) before visualization using a laser scanning confocal microscope (Olympus Fluoview FV1200) with a 150x objective (Olympus UApO N 150xOTIRF, 1.45 NA). Colocalization analysis was completed using the JACoP plugin⁶ for ImageJ.

Traction force microscopy

Glass bottom 35 mm cell culture dishes (World Precision Instruments, FD35-100) were treated with 0.5% 3-aminopropyl-trimethoxysilane (Sigma Aldrich, 281778-100mL) in ddH₂O for 15 minutes, washed with dH₂O, then treated with 0.5% glutaraldehyde (Electron Microscopy Sciences) in 50mM HEPES buffer (Cellgro, 25-060-C1) for 45 minutes. The two treatments allow the polyacrylamide substrate to attach firmly to the dish. Fluorescent bead-imbedded polyacrylamide substrates were made by first thoroughly mixing 30 μ L of 0.25 μ m beads

(Invitrogen, F8810, λ 580/605 nm) with 1670 μL of ddH₂O and 30 μL of 100 mM NaOH. The mixture was then sonicated for 10 minutes at room temperature, and 187.5 μL of 40% polyacrylamide (Fisher Scientific, BP14021) was added along with 94 μL of bis-acrylamide solution (Fisher Scientific, BP1404-250). Fresh 4-5% w/v ammonium persulfate solution was made by dissolving ammonium persulfate (Fisher Scientific, BP179-25) in water, and 150 μL of the solution was then added and mixed by vortex. Finally, 0.5 μL of TEMED (Fisher Scientific, BP150-20) was added and the solution was mixed quickly before being pipetted in 30 μL drops onto the center of each treated microscope dish. The drops are covered immediately with 70% ethanol-washed 18 mm glass coverslips (Fisher Scientific, NC0205777) to create flat substrates.

After the gels have fully polymerized, ~2 mL of 50 mM HEPES buffer was added to each dish prior to the removal of the coverslips with fine-tip tweezers. As cells do not attach well to polyacrylamide, a modified version of the method described by Wang YL and Pelham RJ⁷ was used to modify the gel surface. After as much of the buffer as possible was removed with a vacuum, 200 μL of 1 mM sulfo SANPAH (Thermo Scientific, 22589) was pipetted onto each gel surface. The dishes were left uncovered and irradiated with a UV germicidal lamp for 5 minutes. After the color of the solution has changed from orange to dark brown, indicating photoactivation, the darkened solution was aspirated and the procedure was repeated. The substrates were washed twice for 30 minutes each with 50 mM HEPES buffer to remove residual sulfo-SANPAH. Fibronectin (Fibronectin from bovine plasma, Sigma Aldrich, F1141) was diluted to 0.2 mg/ μL and 50 μL of the solution was added to each activated substrate. An ethanol-washed coverslip was then placed on top of each gel to ensure coverage of the entire gel with fibronectin. The dishes were sealed with Parafilm and left overnight at 4 °C to allow

fibronectin to covalently link to the substrate. The substrates were then washed with DPBS (Gibco® DPBS, Life Technologies, 14040-133). The procedure is summarized in figure 1.

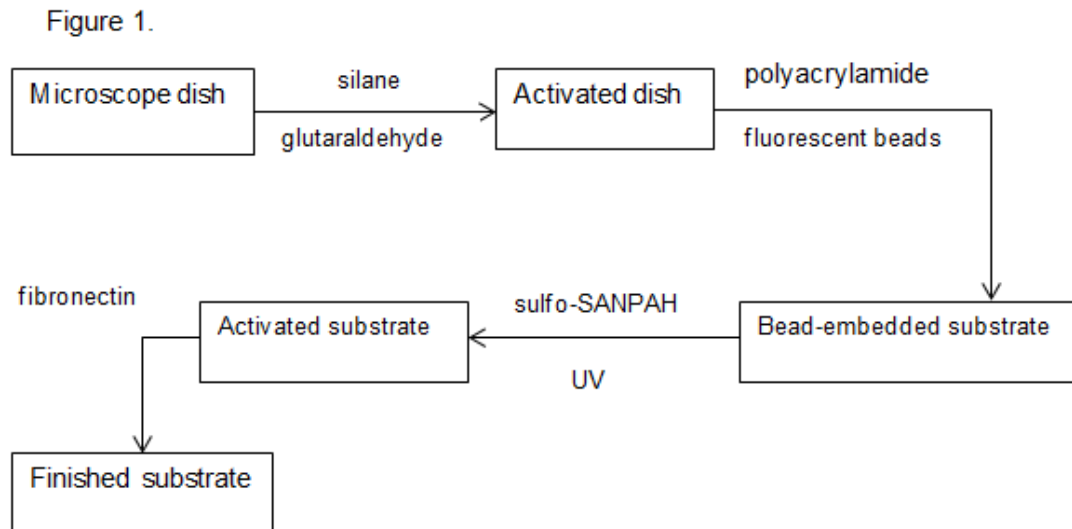


Figure 1. Simplified diagram of substrate preparation

MEF (mouse embryonic fibroblast) cells stably transfected with lifeact-GFP were plated on the substrates. After 24 hour incubation to allow the cells to spread, the dishes were placed under live recording in a spinning disk confocal microscope (Olympus DSU) using a 40x silicone-immersion objective (Olympus UPlanSApo40xS) and under low laser illumination to avoid photobleaching and phototoxicity. Cells were detached by aspirating the growth medium, washing with warm DPBS, then incubating with warm trypsin (Gibco 25300-054). The movement of the fluorescent beads within the substrates was recorded; however, actual tractions have not been calculated at this point. After the cells have detached from the substrate, ~2 mL of growth medium was added to neutralize the trypsin. The cells were then imaged to confirm whether they have completely rounded.

Live cell detachment with drug treatments

CHO cells stably transfected with lifeact-GFP were plated on glass-bottom dishes and allowed to spread for 24 hours. Prior to live-recording on the microscope, the cells were incubated in media containing different drugs: 5 μ M blebbistatin, 10 μ M blebbistatin, 10 μ M Y-27632, 200 nM wortmannin, and 5 μ M s-nitro blebbistatin (Cayman Chemical 13013, 10005583, 10010591, and 13891). Cells were recorded and detached using the same procedures as the traction force microscopy experiments. A laser scanning confocal microscope (Olympus Fluoview FV1200) was used instead of a spinning disk confocal. In order to maintain constant drug concentrations, all reagents used for each group contained the same concentration of the same drug (for example, the 10 μ M blebbistatin group was washed with PBS containing 10 μ M blebbistatin and incubated with trypsin containing 10 μ M blebbistatin). Due to the light-sensitive nature of blebbistatin, only the DIC image for the blebbistatin groups was recorded with a laser emitting in the dark-red region of the spectrum. The rounding time for each cell was determined to be the amount of time between the addition of 250 μ L of trypsin to the dish and the retraction of all major protrusions on the periphery of the observed cell.

Results

Rounding cells sometimes exert inward tractions

During detachment, cells previously attached to a surface cease to exert traction forces on their substrates. Since spread cells exert inward tractions on their substrates, we expected that traction force microscopy will show beads moving away from the approximate center of the cell

during detachment due to the decrease in inward tractions. We observed this outward bead displacement in all cases (figure 2, left). Unexpectedly, we also observed cases of embedded beads moving toward the centers of cells before detaching and rounding (figure 2, right). This inward displacement of beads indicates that, in these instances, the cells exerted inward traction forces before detaching and rounding.

Figure 2.

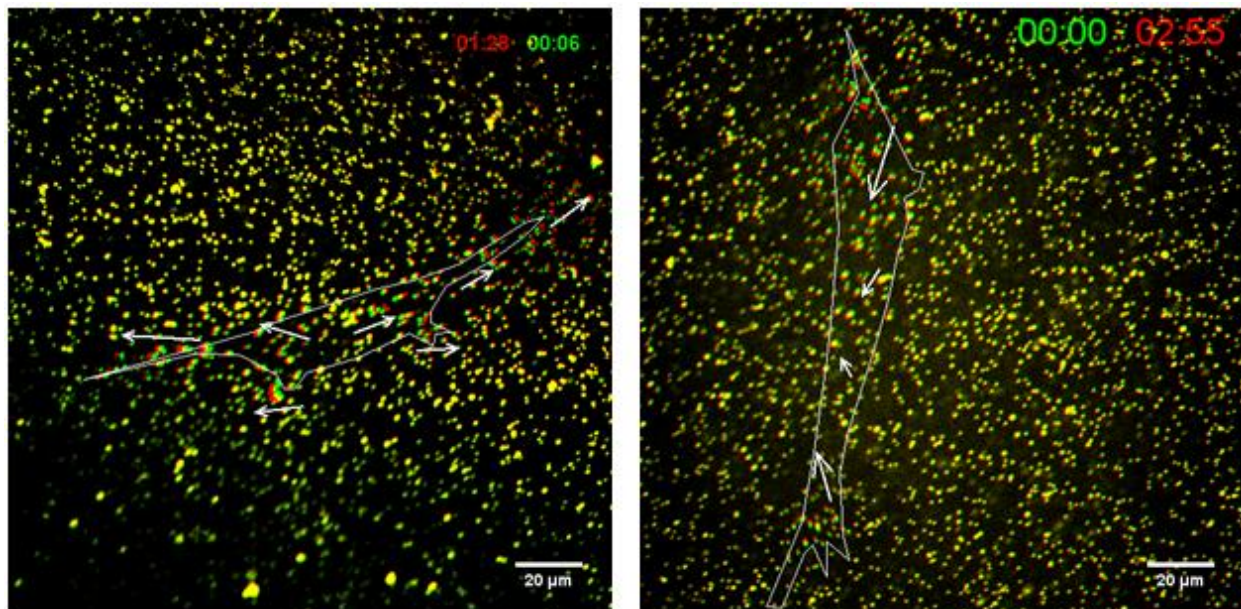


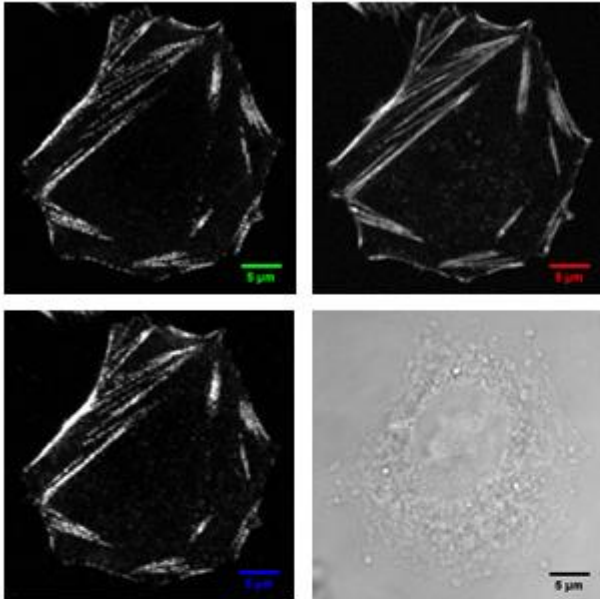
Figure 2. TFM images with initial frames (green) superimposed frames taken at a later time (red). The cells are outlined and bead movements indicated by arrows. During cell detachment and rounding, beads in the elastic substrate moved away from the cell (left). In some cases, beads were observed to move toward the centers of cells immediately prior to detachment and rounding (right), indicating that these cells exerted inward pulling forces on their substrates before rounding.

NMIIB becomes more co-localized with actin and less co-localized with NMIIA at cell periphery during rounding

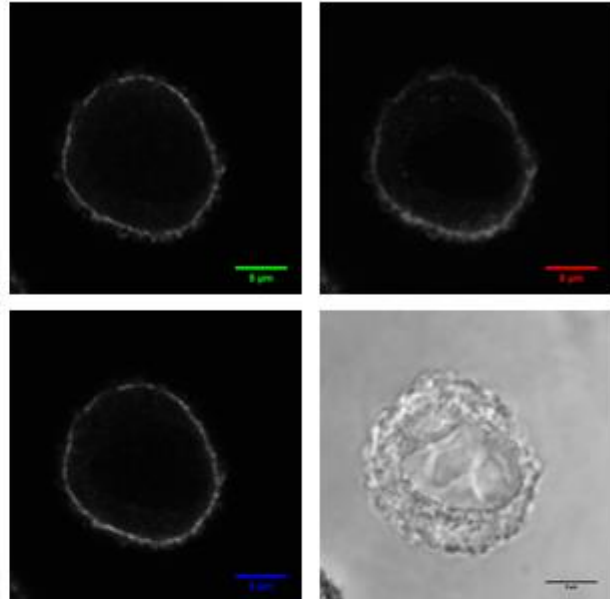
Co-localization analysis of images produced using immunofluorescence (figure 3) indicated a decrease in correlation between NMIIA and actin ($p = 0.03$, $n = 10$, figure 4), while there was also a decrease in correlation between NMIIB and actin, it was not statistically significant ($p = 0.06$, $n = 10$, figure 4). It was apparent that both isoforms of myosin II correlates highly with actin in stress fibers (figure 3). To exclude the effects of stress fiber dissolution the results of the co-localization analysis, parts of the micrographs at the peripheries of the cells were cropped and analyzed (figure 5, 6). Near the cell membranes, the correlation between NMIIA and actin did not change with rounding ($p = 0.43$, $n = 12$, figure 6), but the correlation between NMIIB and actin increased ($p = .006$, $n = 12$, figure 6). NMIIA and NMIIB became more co-localized after rounding ($p = 0.03$, $n = 10$, figure 7). However, at the periphery of the cell, the two isoforms became less correlated ($p = 0.05$, $n = 11$, figure 7).

Figure 3.

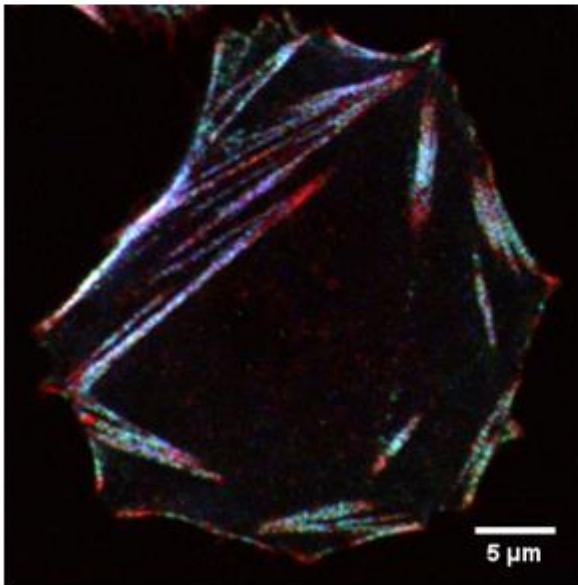
A.



B.



C.



D.

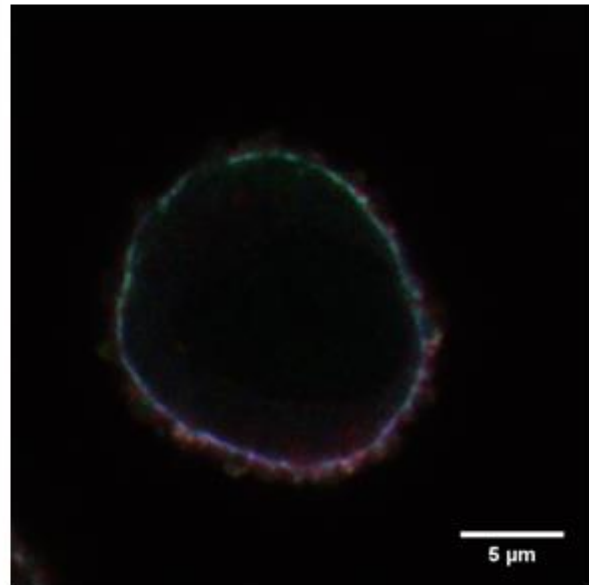


Figure 3. Sample immunofluorescence images of spread (A, C) and rounded (B, D) CHO cells. Individual channels (A,B) of the composite contain scale bars corresponding to their colors in the merged images (C, D). Green: NMIIA, red: actin, blue: NMIIB. All scale bars are 5 microns. DIC is not shown in merged images.

Figure 4.

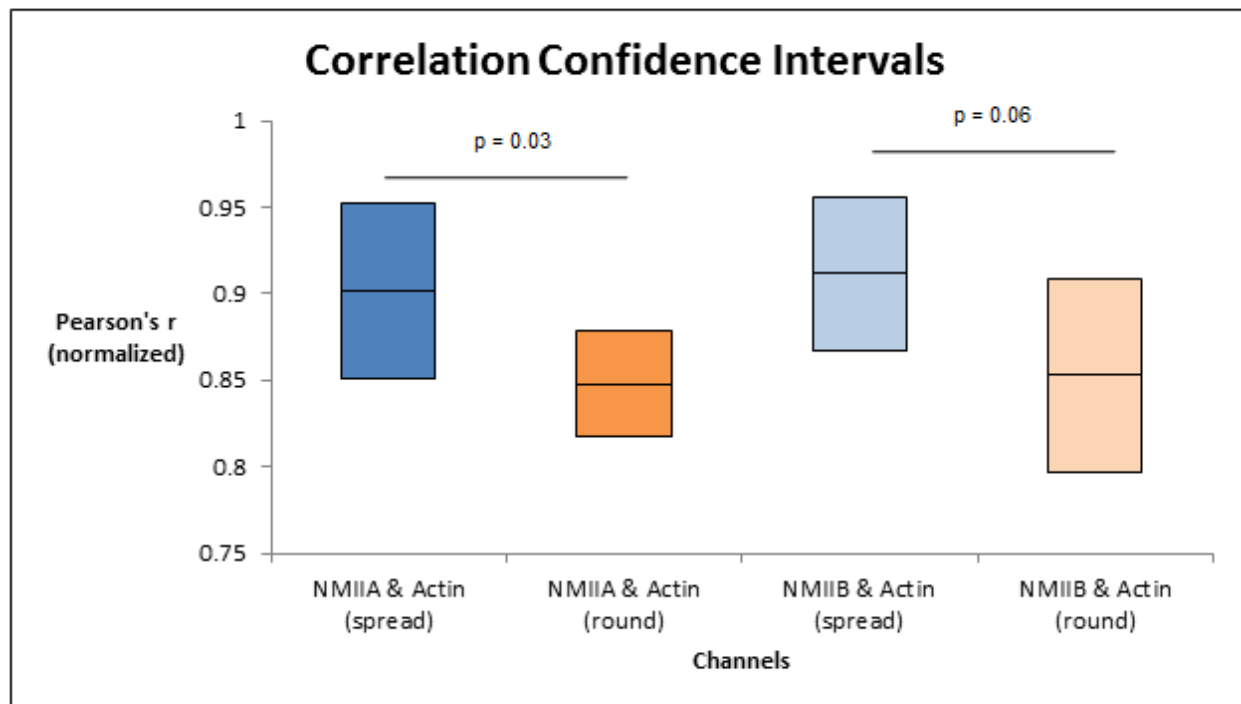


Figure 4. Colocalization analysis indicates that the correlation between NMIIA and actin are different in spread and rounded cells ($p = .03$, $n = 10$); correlation of NMIIIB with actin between spread and rounded cells did not change in a statistically significant manner ($p = .06$, $n = 10$)

Figure 5

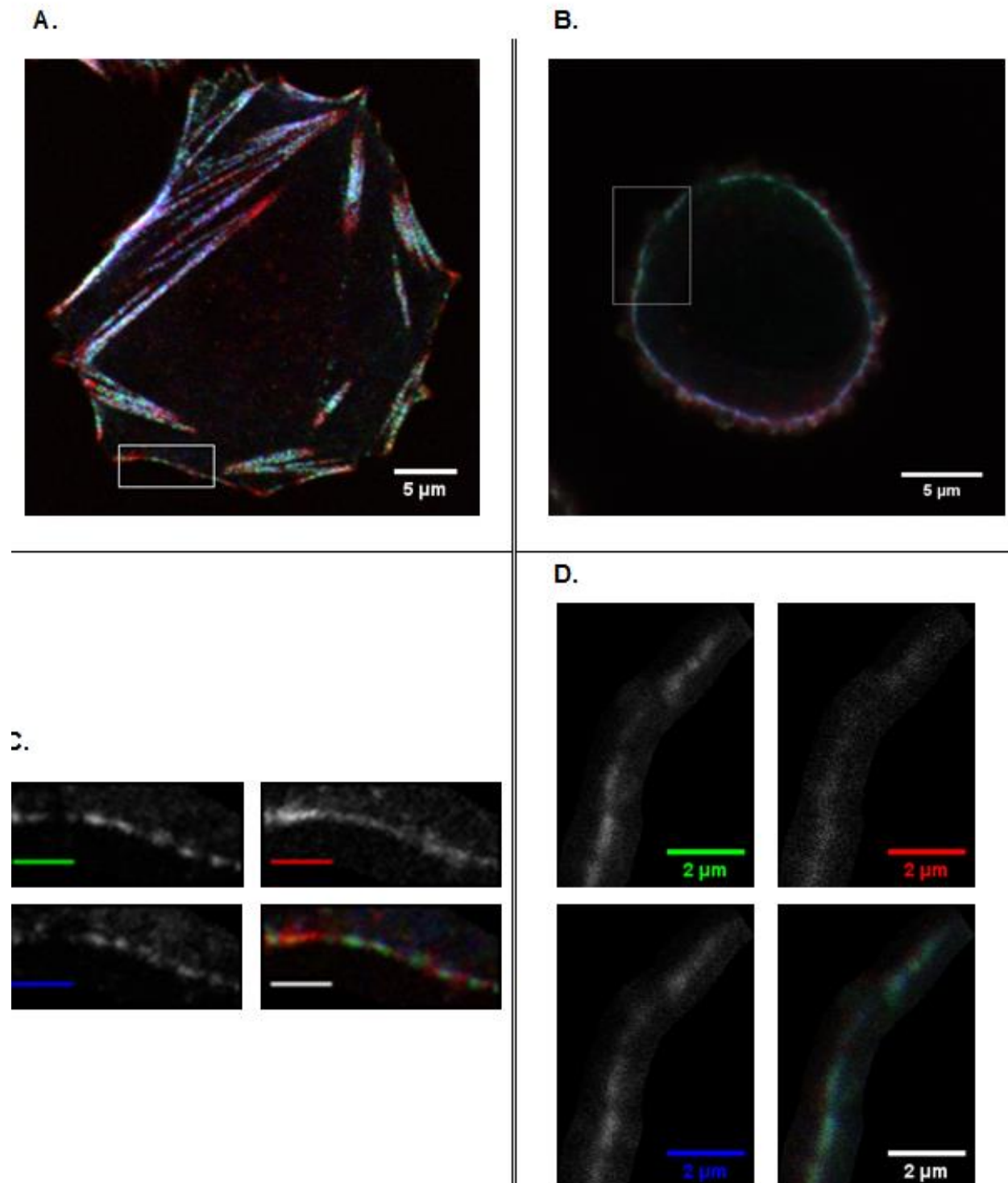


Figure 5. Sections of the peripheries of spread (A,C), and rounded (B,D) CHO cells were selected for co-localization analysis as indicated by the boxes in A and B. Colors of the scale bars correspond to the colors of the channels in merged images, (green: NMIIA, red: actin, blue: NMIIB). Unlabelled scale bars in C are 2 microns.

Figure 6.

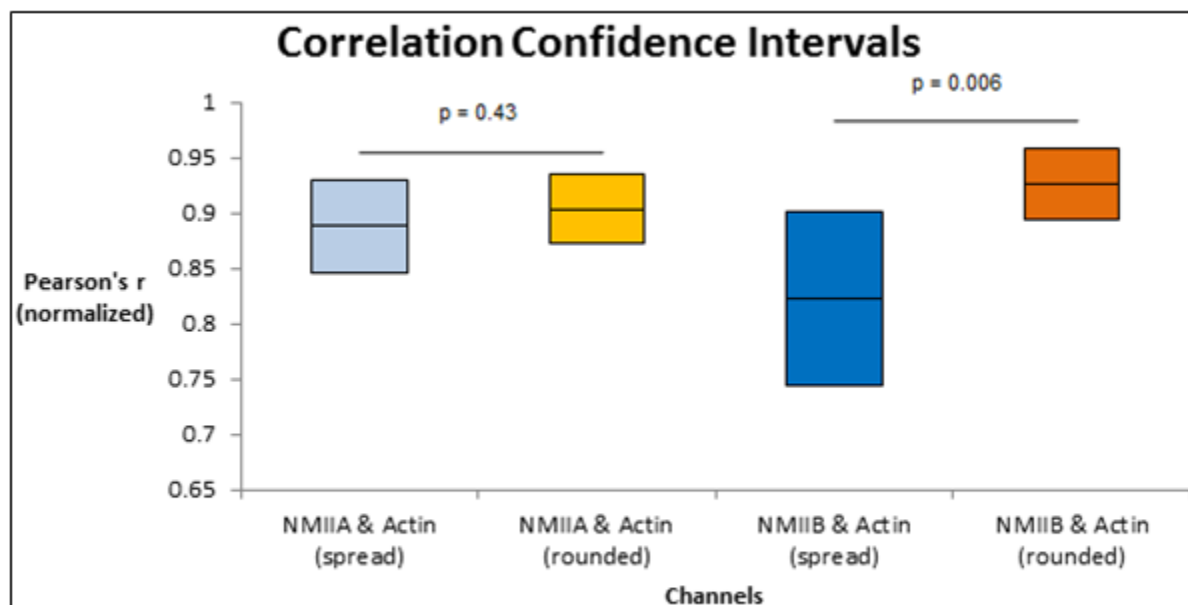


Figure 6. Correlation analysis of the periphery of the cells shows no change in colocalization of NMIIA with actin ($p = 0.43$, $n = 12$) and increase in correlation of NMIIIB with actin in rounded cells ($p = .006$, $n = 12$).

Figure 7.

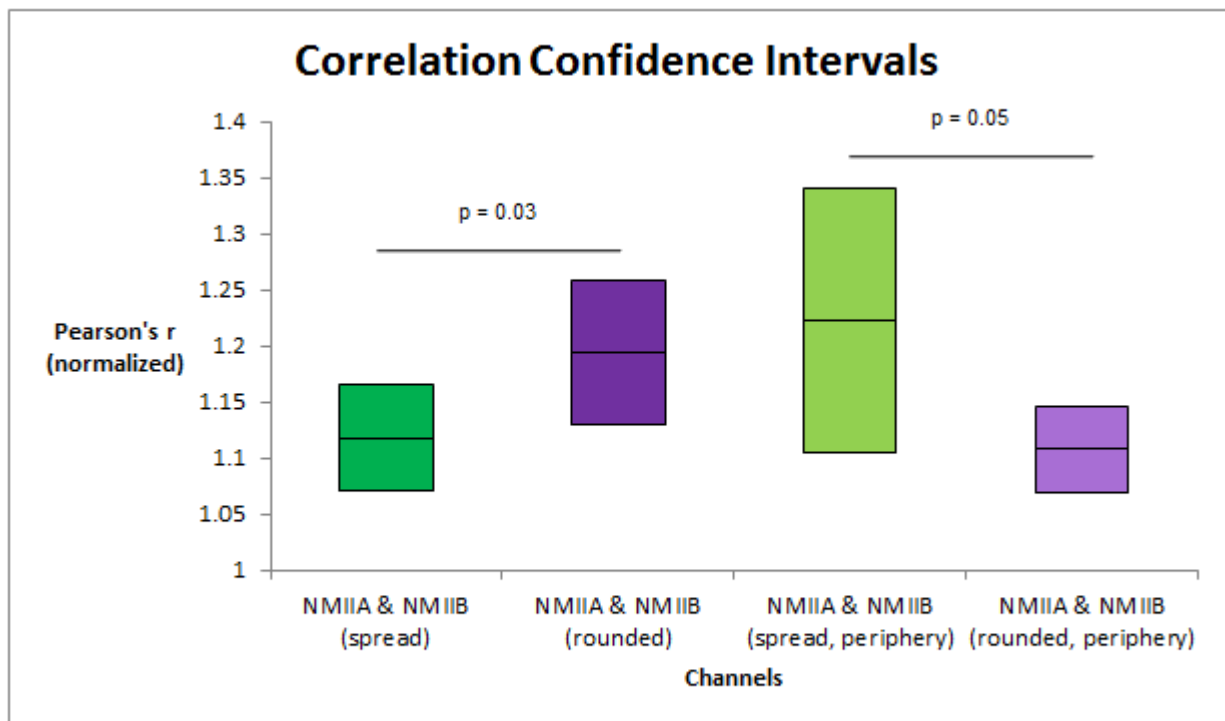


Figure 7. NMIIA and NMIIIB became more correlated after rounding ($p = 0.03$, $n = 10$), but the opposite is true near the cell membrane ($p = 0.05$, $n = 11$).

Inhibition of myosin II disrupted normal detachment-induced cell rounding

Drug treatments caused changes in the time it took for cells to detach and round in response to trypsin. An example of a typical cell undergoing detachment-induced cell rounding is shown in figure 8. Treatment with 200 nM Wortmannin decreased average rounding time ($p = 0.04$, $n = 81$), whereas 10 μ M Y-27632 ($p = 0.001$, $n = 70$), 5 μ M s-nitro blebbistatin ($p < 0.001$, $n = 62$), 5 μ M blebbistatin ($p < 0.001$, $n = 64$), and 10 μ M blebbistatin ($p < 0.001$, $n = 40$) increased the rounding time (figure 9, $n = 77$ for control). The distribution of the time it took the cells to round also changed with drug treatments. The 200 nM Wortmannin group had an approximately normal distribution of rounding times centered around the mean (figure 10). Cells treated with 10 μ M blebbistatin produced a heavily skewed

distribution of rounding times, with few cells rounding relatively early and most of the cells taking several times as long to round (figure 10). The control and 10 μM Y-27632 groups had bimodal distributions, (figure 10) as well as the 5 μM blebbistatin and 5 μM s-nitro blebbistatin groups (not shown). The use of s-nitro blebbistatin was intended to enable visualization of actin with a $\lambda = 488 \text{ nm}$ laser. However, it was observed to be unstable at the conditions used.

Figure 8.

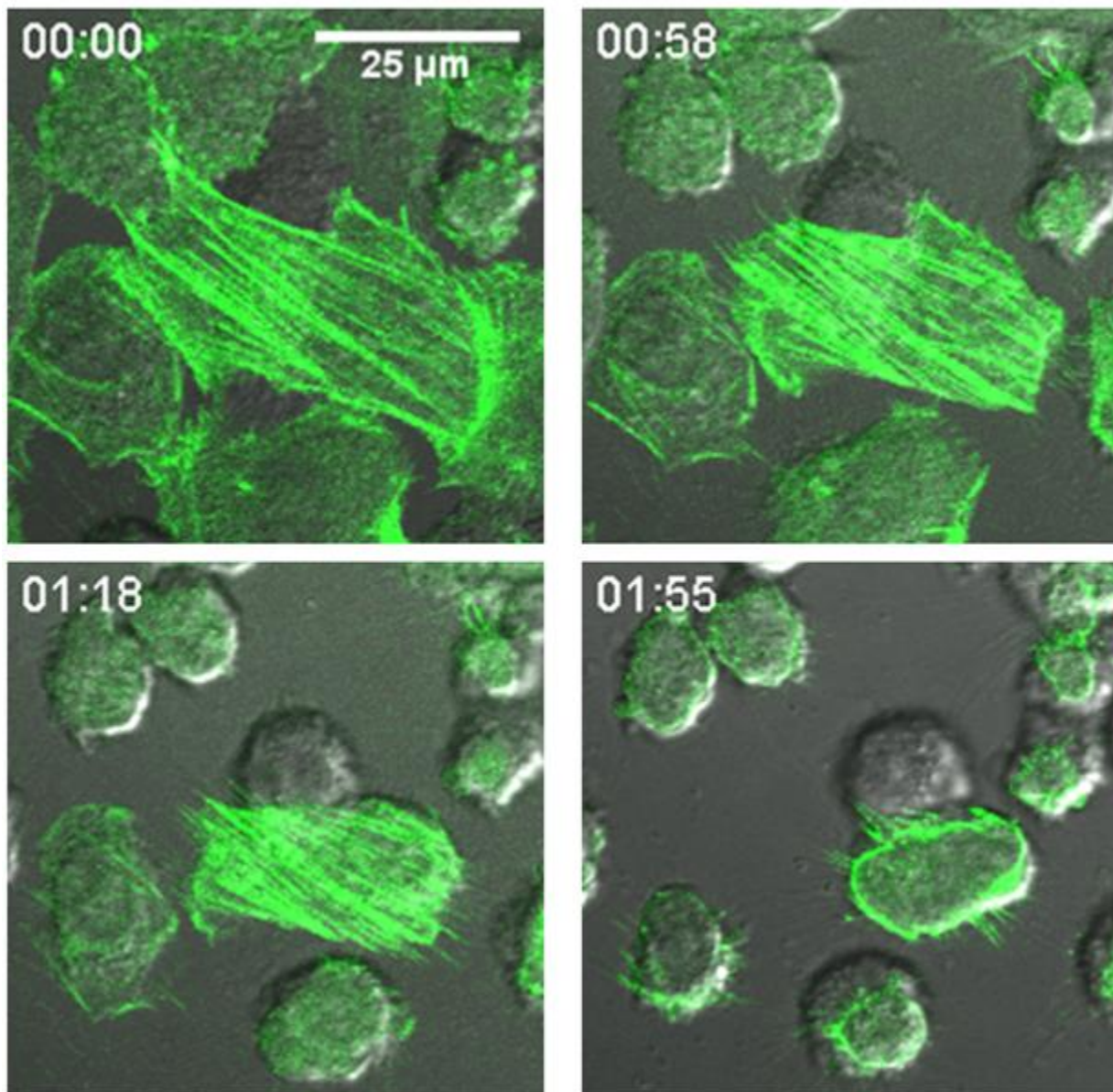


Figure 8. Example of cell rounding. CHO cells attached to a petri dish were detached by treatment with trypsin, which caused rounding. Actin (lifeact-GFP, green) superimposed on DIC

Figure 9.

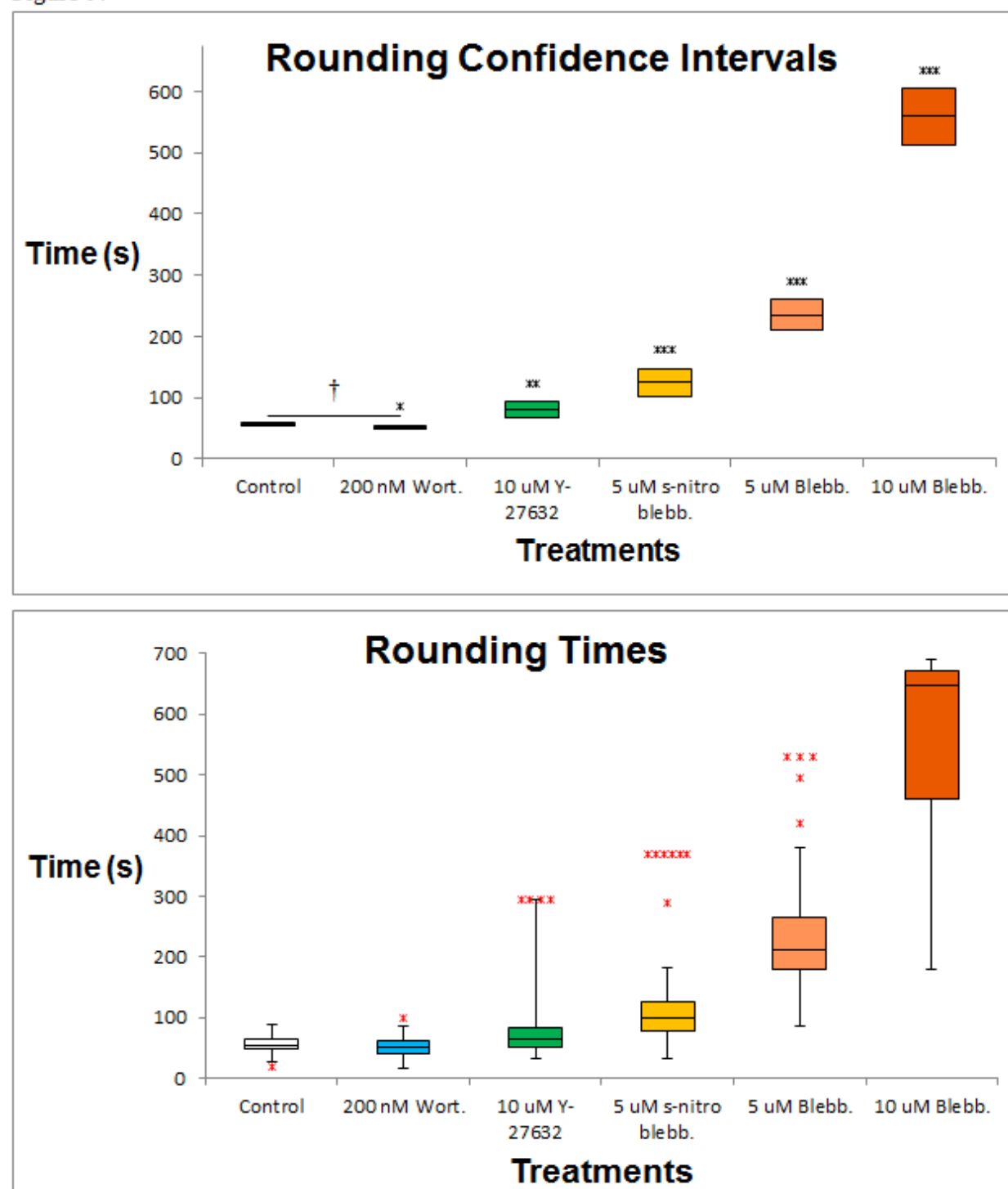


Figure 9. Confidence intervals (top) and box and whisker plots (bottom) of cell rounding times with drug treatments. (top only, compared to control, *: $p \leq 0.05$, **: $p \leq 0.001$, ***: $p < 0.001$, †: confidence intervals overlap)

Figure 10.

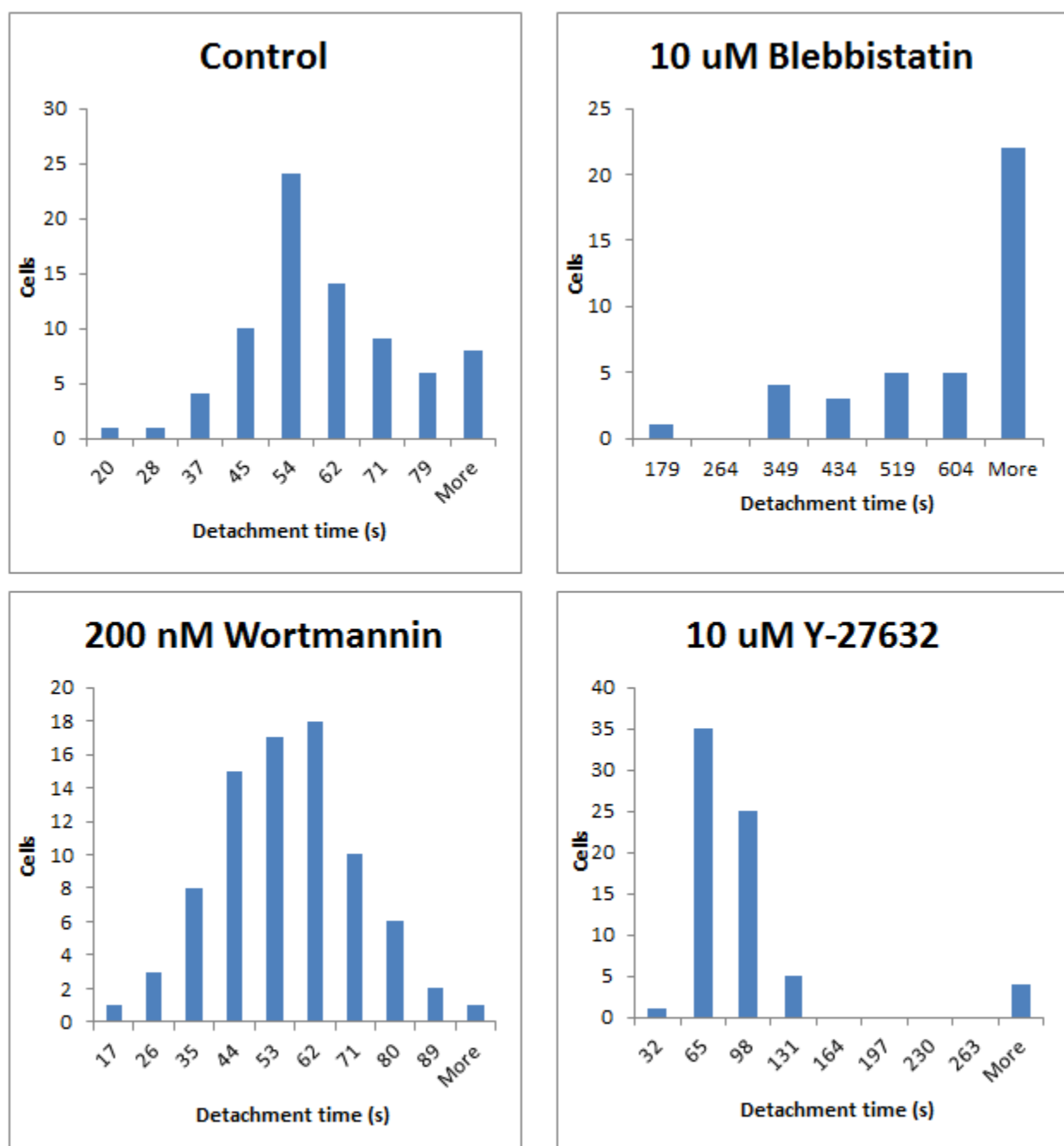


Figure 10. Histograms of cell rounding times for control group and cells treated with 10 μ M blebbistatin, 200 nM Wortmannin, and 10 μ M Y-27632. Distributions of rounding times for 5 μ M blebbistatin and 5 μ M s-nitro blebbistatin (not shown) are similar to that of the control in shape.

Discussion

Detachment-induced rounding involves an active process

Although most cells observed in traction force microscopy rounded quickly and produced only outward bead displacements, some cells rounded slowly and produced inward bead movement before rounding. The cells that were observed to produce inward tractions took several times as long to round and only pulled on their substrates immediately before large-scale detachment and rounding events. One hypothesis that explains the temporary inward bead displacements is that as cells begin to detach from their substrates, the tractions become concentrated on the remaining points of attachments, resulting in inward displacements at those spots. One would also expect outward bead displacements at locations where the integrins were cleaved by trypsin. However, we observed only inward movement of beads in the substrate during the pulling events (figure 2), which suggest that the cells were exerting inward traction forces on their substrates via an active process. All the cells observed to have generated inward traction rounded relatively slowly. Since around six seconds elapsed between each frame of the image stack, the pulling event may have simply happened too quickly to be observed during a typical cell rounding.

Non-muscle myosin II is required for normal detachment-induced cell rounding

Since TFM results suggest that rounding cells generate an inward force, drug treatments were used to identify potential sources of this force. It is known that myosin II is important in mitotic cell rounding.³ To determine whether myosin II is also required for detachment induced cell rounding, we detached CHO cells treated with blebbistatin and observed subsequent

rounding events. Blebbistatin inhibits myosin II when it is detached from actin, and therefore does not lead to an increase in the rigidity of the actomyosin cortex,⁸ which can affect cell rounding.² We found that cells treated with 10 μ M blebbistatin took around ten times as long to round as the control (figure 9). The distribution of rounding times shows that most cells in the control group had rounding times following an approximately normal distribution, with a small number of cells not rounding; in contrast, the 10 μ M blebbistatin group produced a highly skewed distribution, with few cells rounding relatively early and large number of cells taking more ten times as long to round as the control (figure 9).

Researchers have determined that RhoA and Rho-kinase are required for mitotic cell rounding.² To determine whether detachment-induced rounding also proceeds through this pathway, cells were treated with Y-27632 and detached with trypsin. Y-27632 is a Rho-kinase inhibitor. Although we observed a statistically significant increase in mean rounding time, the average rounding time was only around 140% of the control, compared to more than 400% with 5 μ M blebbistatin and ~1000% for 10 μ M blebbistatin (figure 9). It is also worth noting that since all rounding times were produced from one experiment, the statistical significance of the increase in rounding time with Y-27632 treatment may be exaggerated. There are several possible explanations for the relatively small effect of the Rho-kinase inhibitor. The cells may not have been treated long enough to significantly inactivate Rho-kinase. The concentration of the drug also may have been inadequate. Alternatively, compensatory mechanisms may exist that reduces the effects of inactivating Rho-kinase on detachment-induced cell rounding.

Wortmannin, a potent inhibitor of PI3K ($IC_{50} = 3$ nM)⁹ and an inhibitor of myosin light chain kinase (MLCK, $IC_{50} = 170$ nM)¹⁰ did not produce an increase in rounding time when used at 200 nM. Similar to the case with Y-27632, this result may be due to insufficient effective drug

concentration or incubation time during the experiment or the existence of compensatory mechanisms.

NMIIA and NMIIB may perform different roles during detachment-induced rounding

To investigate whether NMIIA and NMIIB perform different functions during detachment-induced cell rounding, we labelled the two isoforms in spread and rounded cells and performed colocalization analysis. We found that the correlation between actin and the two isoforms decreased after rounding (figure 3). Both NMIIA and NMIIB are highly correlated with actin in stress fibers. To exclude the effects of the dissolution of stress fibers on correlation values, we then analyzed only sections of the peripheries of cells (figure 4). On the cell peripheries, the correlation between NMIIA and actin did not change after rounding, whereas the correlation between NMIIB and actin increased (figure 4). While correlation between the two isoforms increased for rounded cells, excluding the stress fibers resulted in a decrease in correlation between NMIIA and NMIIB at the periphery ($p = 0.05$, figure 5). Researchers have found that despite having the same molecular functions (ATP-dependent contraction of F-actin), NMIIA and NMIIB have different localizations in motile cells⁵ and functions in thrombin-induced cell rounding.¹¹ Our results are consistent with NMIIA and NMIIB having different roles in detachment-induced rounding. The decrease in their correlation at cell periphery in rounded cells indicates that the two isoforms adopted more different localizations during rounding, indicating different functions. The increase in correlation between NMIIB and actin may be a result of either increased concentration of NMIIB and actin near the cell periphery from stress fiber dissolution or NMIIB playing an active role in cell rounding at the edges of cells.

Limitations and further study

While the results above suggest that NMIIA and NMIIB have different functions in detachment-induced cell rounding, further experiments are needed to provide conclusive evidence. Tracking the two isoforms in live cells during rounding using transient transfections of NMIIA and NMIIB labelled with photoactivatable GFP can provide further insight into how the two isoforms contribute to rounding. Drug treatment with labelled myosin II heavy chains will show the effect of the treatments on each isoform in live cells. Knockdowns and knockouts (if possible) will show whether each isoform is necessary for detachment-induced rounding and potentially highlight the functions of each. Potentially, spatially localized loss of function using Chromophore Assisted Laser Inactivation (CALI) could be employed, and global knockdowns or CALI studies should be accompanied by full traction mapping to illuminate details of the process. Sandquist et al. showed that NMIIA is required for Rho-kinase mediated rounding after thrombin treatment.¹¹ It would be interesting to observe whether trypsin treatment, which causes more rapid detachment, replicates previous findings with thrombin. As mentioned before, repeat experiments are needed to confirm the effects of various drug treatments on rounding times. Maddox et al. showed that active RhoA increased in cells rounded during mitosis and as a result of a variety of chemical and mechanical treatments, including trypsinization, suggesting the involvement of RhoA in rounding;² therefore, the effects Y-27632 treatment in particular need to be confirmed.

Whereas several of the previous studies involving rounding quantified rounding by recording aspects of cell morphology after treating cells with stimuli known to cause rounding,^{2, 10} this study used the amount of time cells took to round after the rounding stimulus (trypsinization) instead. This difference in methodology may partially explain the different

findings with regards to the effect of the Rho-kinase inhibitor Y-27632. It is also worth noting that while NMIIA and NMIIB change in the degree of correlation with each other after rounding, the two isoforms remain highly co-localized with each other and actin. The two isoforms are known to form heterodimers.⁴ There exists the possibility that NMIIA and NMIIB interact with each other during rounding, complicating their roles during such events. It is also possible that trypsin may trigger one or more signaling pathways in the cell, which would further complicate findings.

Conclusion

This study shows that detachment-induced rounding is an active process driven by myosin II, with the isoforms NMIIA and NMIIB possibly performing different functions during rounding. Although further research is needed to clarify the mechanism of detachment-induced rounding, the findings of this study will aid in efforts to understand how cells round in response to detachment. This topic is relevant in cases such as when cells change their extent of attachment, resulting in rounding which could aid in dispersal in liquid medium, such as when cancer cells detach from a tissue and enter the bloodstream. Understanding how cell round due to detachment may also give insight into other types of cell rounding, such as mitotic rounding. More generally, the mechanisms of detachment-induced rounding can help in understanding how cells produce large-scales morphological changes, which would lead to better understanding of processes such as amoeboid-type movement of leukocytes.

Acknowledgement

I would like to thank Professor Maryna Kapustina for extensive guidance, advice, and help throughout this project. I thank Professor Ken Jacobson for guidance on the approach of the project, extensive advice on this thesis, and providing the opportunity for completing this project. I thank Professor Amy Maddox for her help and advice on the thesis, and Professor Paul Maddox for being my departmental sponsor. I would also like to thank Dr. Ping Liu, Dr. Laurie Betts, Donna Li, Pratik Patel, and Violetta Weinreb for their help and advice in the lab. I thank Hayden Saunders, Brian Saway, and Pranav Haravu, as well as the rest of the BIOL 692H class for providing helpful feedback on this thesis.

References

1. Hong, Z., Ersoy, I., Sun, M., Bunyak, F., Hampel, P., Hong, Z., Sun, Z., Li, Z., Levitan, I., Meininger, G. A. and Palaniappan, K. (2013), *Influence of membrane cholesterol and substrate elasticity on endothelial cell spreading behavior*. J. Biomed. Mater. Res., 101A: 1994–2004. doi: 10.1002/jbm.a.34504
2. Maddox, A. S. (2003). *Mechanisms of Mitotic Cell Rounding*. Ann Arbor, MI: ProQuest
3. Stewart, M. P., Helenius, J., Toyoda, Y., Ramanathan, S. P., Muller, D. J., & Hyman, A. A. (2011). *Hydrostatic pressure and the actomyosin cortex drive mitotic cell rounding*. Nature, 469(7329), 226-231. doi:10.1038/nature09642
4. Maria S. Shutova, Waldo A. Spessott, Claudio G. Giraudo, and Tatyana Svitkina. (2014). *Endogenous Species of Mammalian Nonmuscle Myosin IIA and IIB Include Activated Monomers and Heteropolymers*. Current Biology Vol 24 No 17, 1958-68
5. Sandquist, J. C., & Means, A. R. (2008). *The C-terminal tail region of nonmuscle myosin II directs isoform-specific distribution in migrating cells*. Molecular Biology of the Cell, 19(12), 5156-5167. doi:10.1091/mbc.E08-05-0533
6. S. Bolte & F. P. Cordelières, *A guided tour into subcellular colocalization analysis in light microscopy*, Journal of Microscopy, Volume 224, Issue 3: 213-232.

7. Yu-Li Wang, Robert J. Pelham Jr., (1998). [39] *Preparation of a flexible, porous polyacrylamide substrate for mechanical studies of cultured cells*. Methods in Enzymology. Academic Press, 1998, Volume 298, Pages 489-496, ISSN 0076-6879, ISBN 9780121821999
8. Kovacs, M., Toth, J., Hetenyi, C., Malnasi-Csizmadia, A., & Sellers, J. R. (2004). *Mechanism of blebbistatin inhibition of myosin II*. Journal of Biological Chemistry, 279(34), 35557-35563. doi:10.1074/jbc.M405319200
9. Powis, G., Bonjouklian, R., Berggren, MM., Gallegos, A., Abraham, R., Ashendel, C., Zalkow, L., Matter, WF., Dodge, J., Grindey, G., (1994). Wortmannin, a potent and selective inhibitor of phosphatidylinositol-3-kinase. Cancer Res. 1994 May 1;54(9):2419-23.
10. Nakanishi, S., Kakita, S., Takahashi, I., Kawahara, K., Tsukuda, E., Sano, T., Matsuda, Y. (1992). *Wortmannin, a microbial product inhibitor of myosin light chain kinase*. Journal of Biological Chemistry, 267(4), 2157-2163.
11. Sandquist, J., Swenson, K., Demali, K., Burrige, K., Means, A. (2006). *Rho kinase differentially regulates phosphorylation of nonmuscle myosin II isoforms A and B during cell rounding and migration*. J Biol Chem. 2006 Nov 24; 281(47):35873-83.